International Journal of Pharmaceutics 560 (2019) 57–64

Contents lists available at ScienceDirect

International Journal of Pharmaceutics

journal homepage: www.elsevier.com/locate/ijpharm

Saporin-loaded CD44 and EGFR dual-targeted nanogels for potent inhibition of metastatic breast cancer in vivo

Jing Chen[a], Hua He[b], Chao Deng[a,*], Lichen Yin[b], Zhiyuan Zhong[a,*]

[a] Biomedical Polymers Laboratory, and Jiangsu Key Laboratory of Advanced Functional Polymer Design and Application, College of Chemistry, Chemical Engineering and Materials Science, Soochow University, Suzhou 215123, People's Republic of China
[b] Institute of Functional Nano and Soft Materials (FUNSOM), Soochow University, Suzhou 215123, People's Republic of China

ARTICLE INFO

Keywords:
Nanogels
Targeted delivery
Epidermal growth factor receptor
CD44
Tumor metastasis
Therapeutic proteins

ABSTRACT

Metastasis poses a long-standing treatment challenge for many cancers including breast cancer. Once spreading out, cell-selective delivery of drug appears especially critical. Here, we report on epidermal growth factor receptor and CD44 dual-targeted hyaluronic acid nanogels (EGFR/CD44-NGs) that afford enhanced targetability and protein therapy for metastatic 4T1 breast cancer in vivo. Flow cytometry in CD44 and EGFR-positive 4T1 metastatic breast cancer cells showed over 6-fold higher cellular uptake of EGFR/CD44-NGs than mono-targeting CD44-NGs. MTT and scratch assays displayed that saporin-loaded EGFR/CD44-NGs (Sap-EGFR/CD44-NGs) was highly potent in inhibiting growth as well as migration of 4T1 cells in vitro, with an IC_{50} of 5.36 nM, which was 1.7-fold lower than that for Sap-CD44-NGs. In 4T1-luc metastatic breast cancer model in mice, Sap-EGFR/CD44-NGs exhibited significant inhibition of tumor metastasis to lung at a small dose of 3.33 nmol Sap equiv./kg. Increasing the dosage to 13.3 nmol Sap equiv./kg resulted in further reduced lung metastasis without causing notable adverse effects. These dual-targeted nanogels with improved cancer cell selectivity provide a novel platform for combating breast cancer metastasis.

1. Introduction

Cancer metastasis presents a main challenge for cancer therapy (Chaffer and Weinberg, 2011; Mehlen and Puisieux, 2006), and over 90% of breast cancer patients died from distant metastasis to different organs (Obenauf and Massague, 2015; Su et al., 2016). The small sized metastatic nodules often have poor vasculature and broad dissemination in invaded organs, thus may not be accessible by many current therapeutic agents (Schroeder et al., 2012). Nano-drugs that are able to target and release therapeutic agents to metastatic sites have emerged as a potent strategy to treat metastatic breast cancers (Landesman-Milo et al., 2015; Schroeder et al., 2012). For example, an albumin-bound paclitaxel (Abraxane®) has been approved to treat metastatic breast cancer (Lluch et al., 2014; Wicki et al., 2015). Nevertheless, the nanomedicines in the clinic are often restricted by relatively low tumor targetability and slow drug release at targeted metastatic sites (Yu et al., 2016b). To boost drug release in cancer cells, pH-sensitive nanoparticles as well as redox-sensitive nanogels were developed to achieve fast release of anticancer agents including paclitaxel, cabazitaxel, doxorubicin, and siRNA upon internalization into cancer cells, resulting in an obvious reduction of primary tumor growth and lung metastasis incidence in 4T1 breast tumor model (Chen et al., 2018; Tang et al., 2017; Xu et al., 2016; Yu et al., 2016a). Meanwhile, some targeting peptides like LHRH, iRGD, and tLyP-1 have been selected and decorated on nanoparticles to promote the cellular uptake of anticancer agents (cisplatin, doxorubicin, docetaxel, etc.) in metastatic breast cancer cells (Hamilton et al., 2015; Han et al., 2017; Li et al., 2015; Liang et al., 2017; Morshed et al., 2016). These active tumor-targeted nano-drugs demonstrated elevated suppression on tumor metastasis in mice bearing 4T1 and MDA-MB-231 tumors in comparison with the counterparts without targeting ligands. Although dual-targeted nano-drugs often provide better tumor selectivity and more efficient target cell uptake (Nan et al., 2017; Qiao et al., 2018; Zhao et al., 2017; Zhu et al., 2018), few of them have been employed to treat tumor metastasis. In addition, chemotherapeutic agents that used for cancer treatment often cause notorious side effects to healthy tissue and organs, and thus largely reduce their therapeutic windows and efficacy. Conversely, protein drugs possess potent anticancer effect, high specificity, and low toxicity, and have recently received growing interests for treatment of various cancers (Dutta et al., 2017; Qiu et al., 2018; Walsh, 2014; Wang et al., 2014). We previously showed that a therapeutic protein (granzyme B) could be efficiently deliver by EGFR and CD44 dual-targeting hyaluronic acid nanogels (EGFR/CD44-NGs), and resulted in nearly complete growth suppression of primary SKOV-3 and MDA-MB-231 tumors in mice, without causing obvious side effects (Chen et al., 2017b).

* Corresponding authors.
E-mail addresses: cdeng@suda.edu.cn (C. Deng), zyzhong@suda.edu.cn (Z. Zhong).

https://doi.org/10.1016/j.ijpharm.2019.01.040
Received 29 November 2018; Received in revised form 10 January 2019; Accepted 15 January 2019
Available online 27 January 2019
0378-5173/

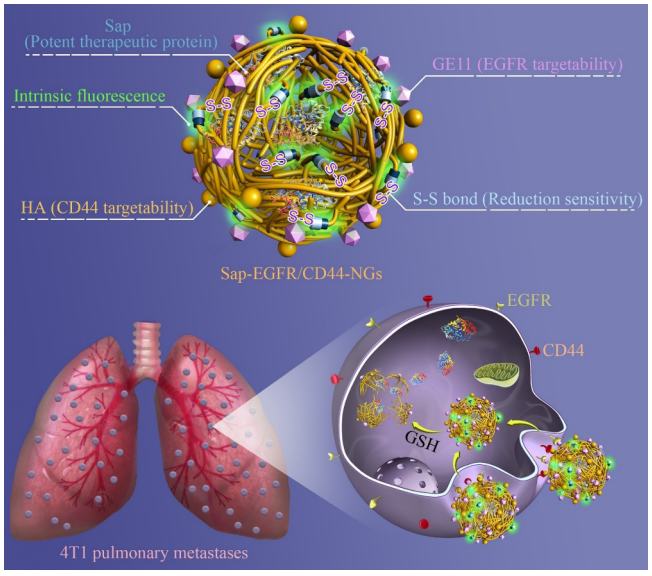

Fig. 1. Schematic illustration of inhibiting breast tumor metastasis to lung in vivo via tumor-targeted delivery of saporin using EGFR and CD44 dual-targeting hyaluronic acid nanogels (EGFR/CD44-NGs).

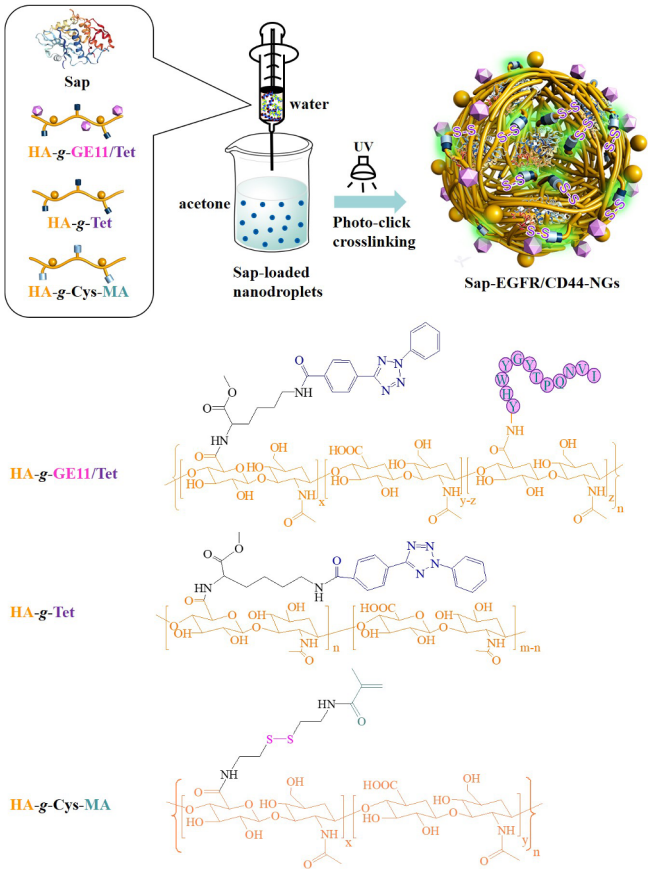

Fig. 2. Preparation of Saporin-loaded CD44 and EGFR dual-targeted hyaluronic acid nanogels (EGFR/CD44-NGs) by combing inverse nanoprecipitation and catalyst-free photoclick reaction.

Here, we report on inhibiting metastatic breast cancer in mice using saporin (Sap)-loaded EGFR/CD44-NGs (Fig. 1). Saporin can irreversibly block protein synthesis in eukaryotic cells and has been advanced into clinical trials to treat different cancers including leukemia that are refractory to traditional chemotherapy (Chang et al., 2017; Kreitman

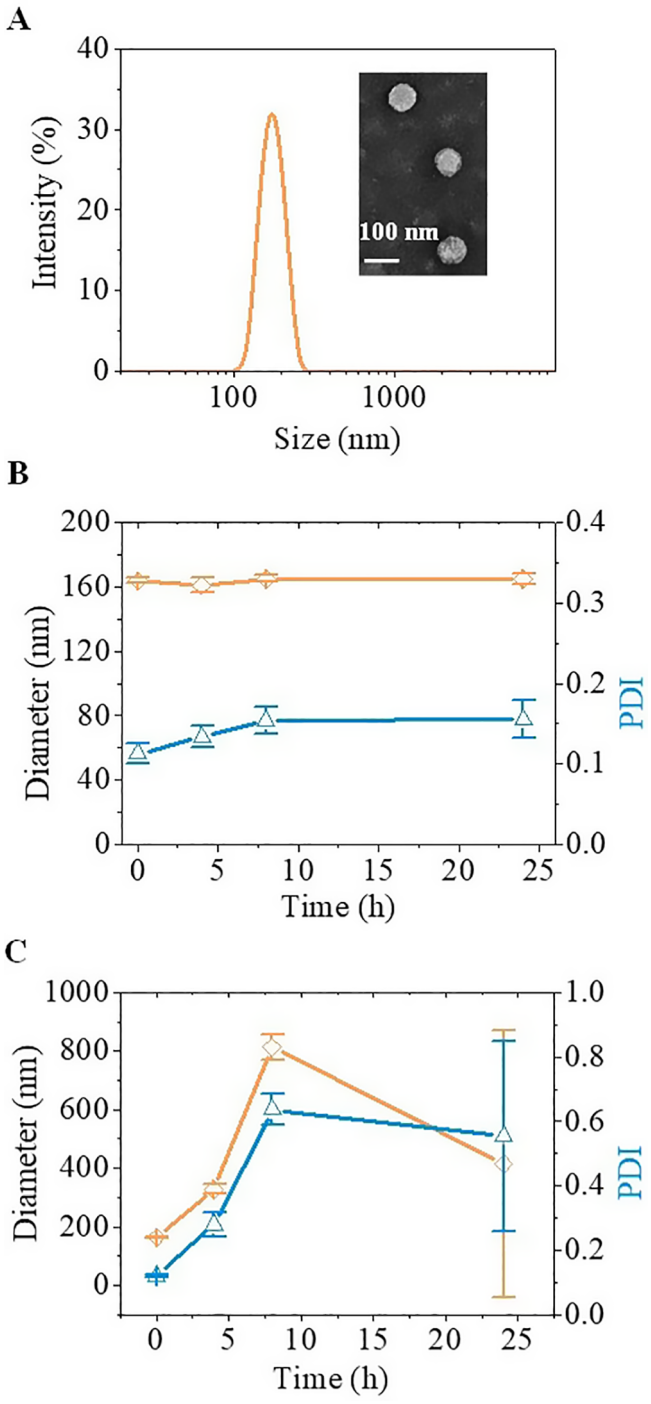

Fig. 3. Characterization of Sap-EGFR/CD44-NGs. (A) Size distribution measured by DLS and TEM. (B) Colloidal stability at a nanogel concentration of 1 mg/mL against 10% FBS. (C) Size changes with time in PB containing 10 mM GSH.

et al., 2001). Nanogels possess watery atmosphere that provides high loading and excellent compatibility with proteins, are thus extremely appealing for protein delivery (Jiang et al., 2014; Li et al., 2017; Vermonden et al., 2012; Zhang et al., 2015). Hyaluronic acid (HA) and GE11 peptide (YHWYGYTPQNVI) are known to target CD44 and EGFR receptors of cancer cells, respectively (Chen et al., 2017a; Hosseinzadeh et al., 2017; Liang et al., 2016; Lim et al., 2018; Rao et al., 2016; Wang et al., 2015). Many metastatic cancer cells like 4T1 and MDA-MB-231 cells have been reported to overexpress CD44 and EGFR receptors (Liu et al., 2012; Morishige et al., 2008; Ravar et al., 2016; Yae et al., 2012;

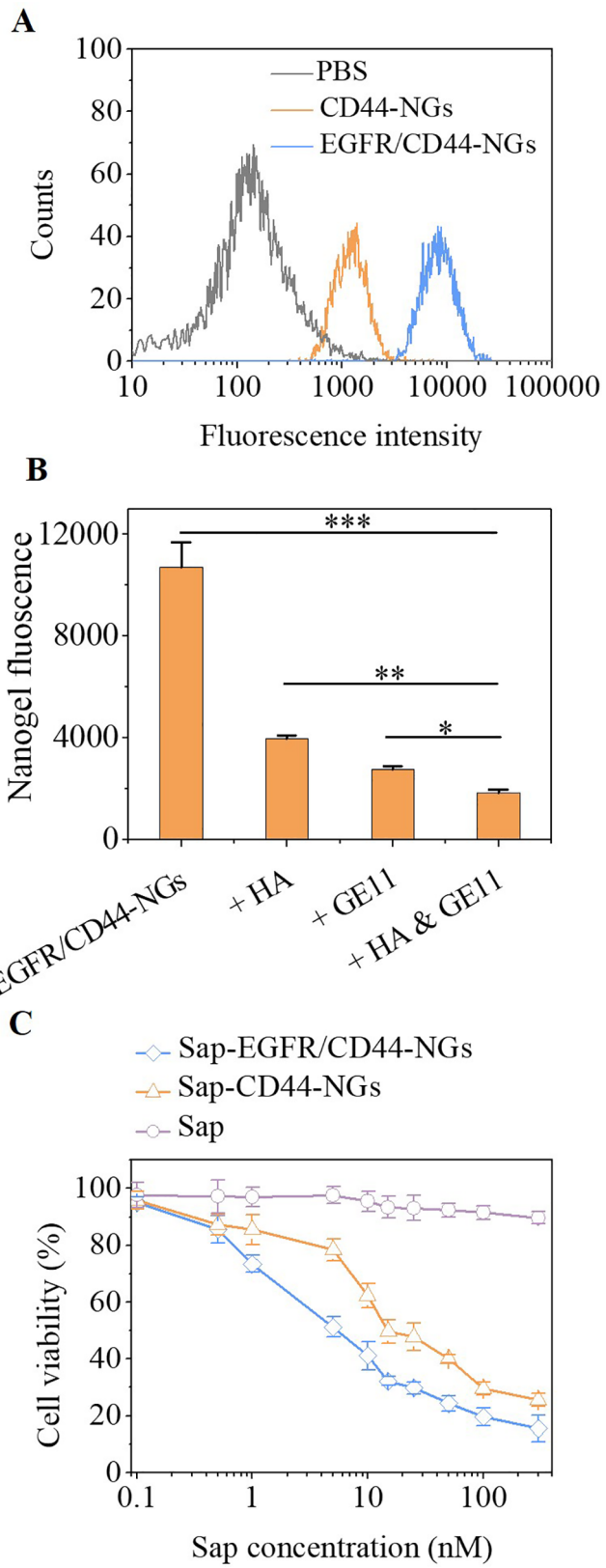

Fig. 4. (A) Flow cytometry assay of 4T1-luc cells treated with CD44-NGs and EGFR/CD44-NGs for 4 h (nanogel concentration: 200 μg/mL). (B) Flow cytometry assay of 4T1-luc cells pre-treated with free HA, GE11 or HA + GE11 for 4 h prior to incubation with EGFR/CD44-NGs. (C) Antitumor activity of Sap-loaded nanogels in 4T1-luc cells. The cells were incubated with Sap-loaded NGs for 4 h, followed by a 92 h culture in fresh medium.

Yang et al., 2009, 2013). The cystamine moieties affords nanogels with reduction-sensitivity, facilitating the swift release of encapsulated Sap in cancer cells. We hypothesized that EGFR/CD44-NGs following the encapsulation of therapeutic proteins could effectively inhibit the metastasis of breast cancers in vivo.

2. Experimental section

2.1. Preparation of saporin-loaded dual-targeting hyaluronic acid nanogels (Sap-EGFR/CD44-NGs)

Sap-EGFR/CD44-NGs were developed by forming nanodroplets via inverse nanoprecipitation technique, followed by covalent crosslinking using catalyst-free "tetrazole-alkene" click chemistry. Briefly, HA grafted with tetrazole (HA-*g*-Tet), cystamine-methacrylmide (HA-*g*-Cys-MA), tetrazole plus GE11 (HA-*g*-GE11/Tet), and saporin (theoretical loading content: 2 wt%) were completely dissolved in PB (pH 7.4, 10 mM) to obtain an aqueous solution (polymer concentration = 1.25 mg/mL). The molar ratios of Tet/MA and GE11/HA were fixed at 1/1 and 0.96/1, respectively. Then, the above aqueous solution (1 mL) following injection to acetone (100 mL) was irradiated with UV (320–390 nm, 50 mW/cm^2) for 3 min. After the removal of the acetone solvent by rotatory evaporator, the protein-loaded nanogels (Sap-EGFR/CD44-NGs) were collected by exhaustive dialysis (MWCO 3500) against D.I. water and freeze-drying. Mono-targeting Sap-CD44-NGs was prepared in a similar way from HA-*g*-Tet and HA-*g*-Cys-MA. Similarly, blank nanogels including CD44-NGs and EGFR/CD44-NGs were fabricated without mixing Sap protein into the aqueous solution of HA derivatives.

2.2. Cell scratch wound healing assays

4T1-luc cells (5 × 10^5 cells/well) were cultured in six-well plates for around 24 h to attain 90% confluence. After abandoning the medium, horizontal mechanical scratch wound was generated using a 10-μL pipet tip. The cells following washing with PBS were incubated with Sap-EGFR/CD44-NGs, Sap-CD44-NGs, blank NGs and PBS. The recovery of cell wound regions was captured at 36 h using an inverted microscope (4× magnification, Olympus). The distance of wound closure was used to evaluate the inhibitory capacity of protein-loaded nanogels on cell movement.

2.3. Transwell migration assay

Cell migration behaviors were investigated using transwell chambers (8 μm pore, 6.5 mm diameter). Briefly, 0.75 mL of RPMI 1640 containing 10% FBS and 0.5 mL of 4T1-luc cells (1 × 10^5 cells/well) in serum-free RPMI 1640 were added into the lower and upper chambers, respectively. Then, the cells in the upper chamber were treated with Sap-EGFR/CD44-NGs or Sap-CD44-NGs (Sap concentration: 300 nM) for 4 h. After removing the culture medium, the cells were further incubated in fresh medium for 44 h. The cells migrated into lower chamber were stained with crystal violet (0.5 wt%) solution in PB. The intensity of violet in cells was measured at 570 nm by microplate reader following dissolving in 50% acetic acid. Blank EGFR/CD44-NGs and PBS were used as negative controls.

2.4. Blood analysis

The mice were handled under protocols approved by the Animal Care and Use Committee of Soochow University. For routine blood test, healthy BALB/c mice (n = 3) were intravenously injected with 0.15 mL of Sap-loaded NGs solution (200 μg Sap equiv./kg) through the tail vein. The blood harvested from the orbital sinus following 24 h administration was used to analyze red blood cell (RBC), white blood cell (WBC), platelet (PLT), hemoglobin (HGB), hematocrit (HCT), mean corpuscular volume (MCV), mean corpuscular hemoglobin

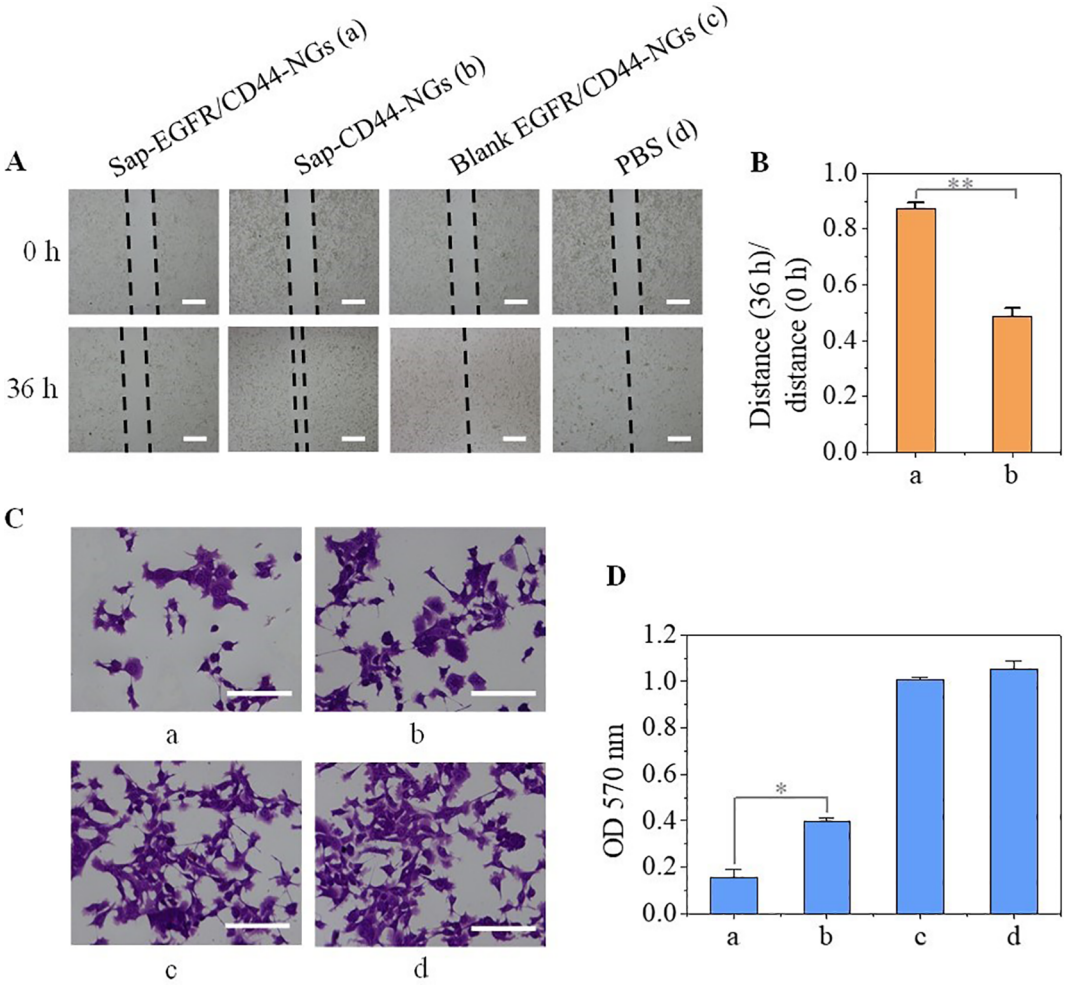

Fig. 5. Cell migration assays. (A) Microscopy photographs of 4T1-luc cells wound scratch treated with (a) Sap-EGFR/CD44-NGs, (b) Sap-CD44-NGs, (c) blank NGs, and (d) PBS. Scale bars = 1 mm. (B) Statistics of scratch distance (n = 3). (C) Transwell migration assay of 4T1-luc tumor cells treated with different formulations. Scale bars = 200 μm. (D) The migrated cells were quantified by microplate reader (n = 3). The intensity of violet staining was measured as absorbance at 570 nm. (For interpretation of the references to colour in this figure legend, the reader is referred to the web version of this article.)

concentration (MCHC), and mean corpuscular hemoglobin (MCH). PBS and blank NGs were used as control groups.

2.5. In vivo antitumor efficacy

4T1-luc metastatic cancer model was established by tail vein injection of luciferase-engineered 4T1 cells (1×10^5 cells in 200 μL PBS) into 6-week old BALB/c mice on day 0. Then, tumor-bearing mice were treated with Sap-EGFR/CD44-NGs (3.33 and 13.3 nmol Sap equiv./kg) and Sap-CD44-NGs (3.33 nmol Sap equiv./kg) in 150 μL of PBS via tail vein on day 5, 9, and 13. The body weight of mice was assessed on day 0, 3, 6, 9, and 13. Lung metastasis was monitored via bioluminescence imaging of BALB/c mice using In Vivo Xtreme imaging instrument (Bruker) on day 5, 9, and 13. D-luciferin potassium salt (150 mg/kg) was intraperitoneally injected 5 min before imaging. Bioluminescence imaging data were processed using the Bruker imaging software. After the last imaging on day 13, all mice were sacrificed under anesthesia. The lung and heart of each animal were resected as a whole, weighed, and injected with 10% formalin into trachea until the lungs inflated. Tumor nodules on lungs (n = 6 per group) were counted under a dissecting microscope. The lung, heart, kidney and liver tissues were embedded in paraffin, sectioned with a thickness of 4 μm, stained with hematoxylin and eosin (H&E), and examined using a digital microscope (Leica Q Win).

3. Results and discussion

3.1. Preparation of Sap-EGFR/CD44-NGs

Sap-EGFR/CD44-NGs were easily prepared from HA-*g*-(Cys-MA), HA-*g*-tetrazole, and HA-*g*-GE11/tetrazole by combining nanoprecipitation and photo-click-crosslinking (Fig. 2), as previously reported for granzyme B-loaded NGs (Chen et al., 2017b). Sap is much less expensive than granzyme B and currently tested for treating refractory leukemia patients (Chang et al., 2017; Kreitman et al., 2001). The loading levels were assessed by microBCA assays, and the results exhibited that almost quantitative loading of Sap (> 99%) was achieved by EGFR/CD44-NGs at a theoretical loading content of 2 wt%. Of note, Sap-EGFR/CD44-NGs exhibited a hydrodynamic diameter of ca. 162 nm, a low polydispersity (PDI) of 0.13 (Fig. 3A), and a negative surface charge of around −15 mV. Sap-EGFR/CD44-NGs in a TEM photograph exposed a spherical structure and an average size of around 100 nm (Fig. 3A), which was smaller than that determined by DLS, owing to dehydration. Remarkably, Sap-EGFR/CD44-NGs demonstrated little changes of size and size distribution against 10% fetal calf serum (FBS) for 24 h at 37 °C (Fig. 3B), signifying their decent stability. Fast and obvious swelling was, however, displayed for Sap-EGFR/CD44-NGs within 8 h under 10 mM GSH (Fig. 3C), suggesting that Sap-EGFR/CD44-NGs possess high reduction-sensitivity.

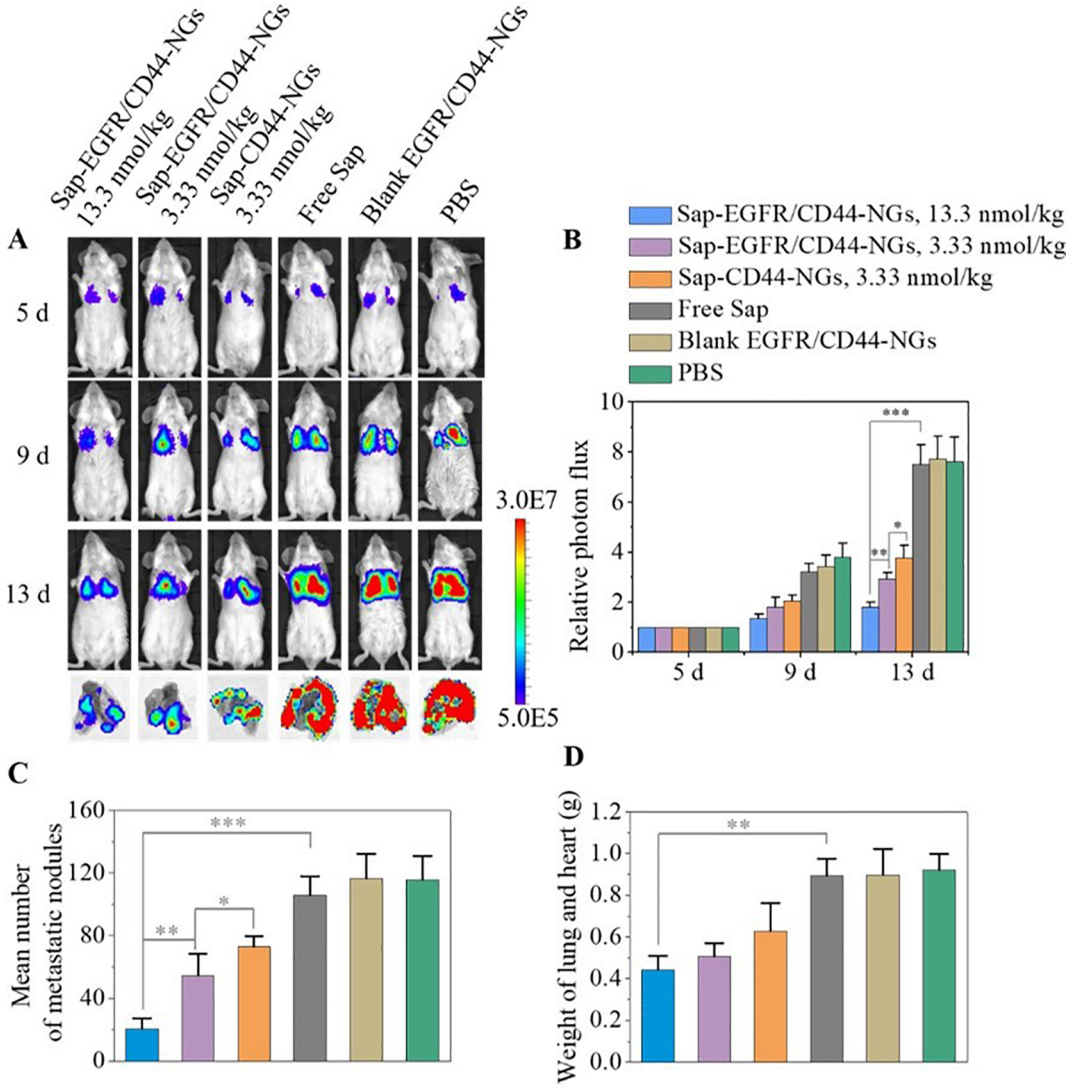

Fig. 6. In vivo inhibition of 4T1-luc breast cancer metastasis by Sap-EGFR/CD44-NGs. (A) Bioluminescence imaging of 4T1-luc tumor metastasis in lung. The bottom row was *ex vivo* imaging of lung blocks harvested on day 13. (B) Quantified average luminescence levels of mice treated with different formulations on day 5, 9 and 13 (n = 6). (C) Average tumor nodules on the lung tissue of mice treated with different formulations (n = 6). (D) Total weight of lung and heart of mice following different treatments (n = 6).

3.2. Cellular uptake and cytotoxicity of Sap-EGFR/CD44-NGs

"Tetrazole–alkene" photo-click hydrogels and nanogels are intrinsically fluorescent (Chen et al., 2016; Fan et al., 2013; Ramil and Lin, 2014). Taking advantage of the intrinsic fluorescence, we studied their cellular uptake using flow cytometry without adding any fluorescent dye. Flow cytometry revealed that EGFR and CD44 overexpressing 4T1 cancer cells following the treatment with dual-targeting EGFR/CD44-NGs exhibited over 6-fold higher nanogel fluorescence intensity than those treated with mono-targeting CD44-NGs (Fig. 4A), corroborating that cellular uptake of CD44-NGs is promoted by introducing GE11 as a second targeting ligand. The dual targeting effect of EGFR/CD44-NGs was further confirmed by inhibition experiments. Pretreating 4T1 metastatic breast cancer cells with HA, GE11, or HA + GE11 resulted in remarkably decreased cellular uptake, in which HA + GE11 group presented significantly lower nanogel fluorescence than both HA and GE11 groups (Fig. 4B).

The antitumor activity of Sap-loaded NGs was evaluated by MTT assays in 4T1-luc cells. The results showed that Sap-EGFR/CD44-NGs were highly potent toward 4T1-luc cells with a low IC_{50} of 5.36 nM, 1.7-fold lower than mono-targeting Sap-CD44-NGs (Fig. 4C). The largely enhanced cytotoxicity of Sap-EGFR/CD44-NGs against 4T1-luc tumor cells signifies the synergistic targeting effect of GE11 and HA. As expected, free saporin revealed minimal toxicity to 4T1-luc cancer cells even at a high protein dose of 300 nM, due to poor protein internalization and intracellular trafficking (Akishiba et al., 2017; Chang et al., 2017; Raghupathi et al., 2017). Similar to previous report for SKOV-3 cells (Chen et al., 2017b), blank nanogels including CD44-NGs and EGFR/CD44-NGs induced little toxicity towards 4T1-luc cells at concentrations 0.5–1 mg/mL (Fig. S1).

3.3. Inhibition of cell migration in vitro

Cancer metastasis is a very complex dynamic biological process consisting of cell adhesion, invasion and migration (Jiang et al., 2017). Cell wound healing technique is a straightforward method for evaluating cell migration and repairing ability (Gao et al., 2017). As shown in Fig. 5A, the cell wound was completely healed following culture with PBS or blank nanogels for 36 h, supporting that 4T1 has excellent migration ability. However, cell wound treated with Sap-loaded nanogels exhibited much slower wound recovery, in which Sap-EGFR/CD44-NGs led to negligible wound healing in 36 h (Fig. 5B). We further evaluated

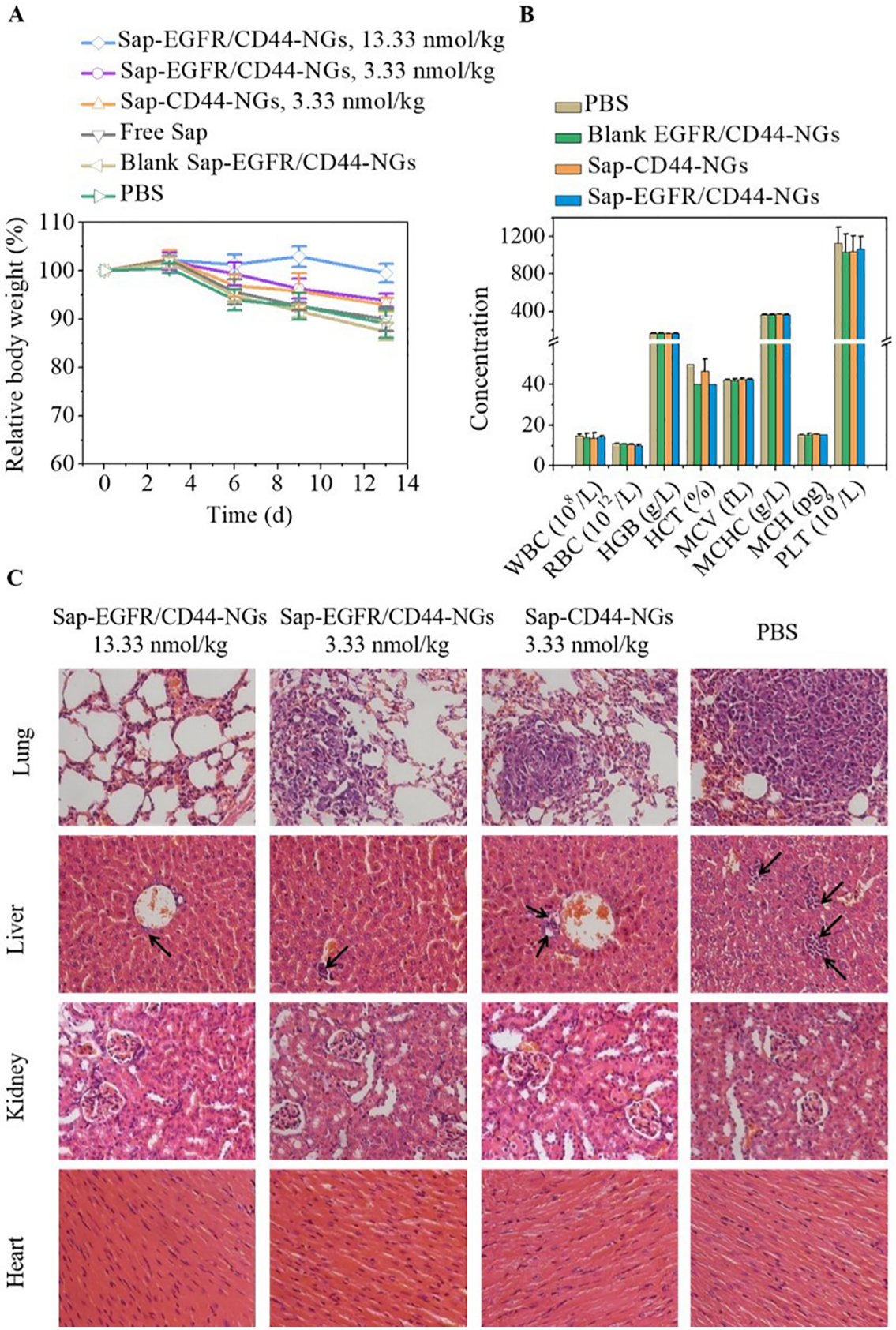

Fig. 7. (A) Relative body weight change of metastatic 4T1-luc breast tumor-bearing mice treated with different formulations in 13 days. (B) Blood analysis of healthy Balb/c mice treated with Sap-EGFR/CD44-NGs and Sap-CD44-NGs at a dose of 13.3 nmol Sap equiv./kg at 24 h post-injection (n = 3). (C) H&E staining of lung, heart, kidney and liver of metastatic 4T1 lung tumor-bearing nude mice treated with different formulations for 13 days. Arrow indicates tumor cells.

the effect of Sap-loaded NGs on inhibiting invasive ability of 4T1 tumor cells using transwell assay. The results displayed that in contrast to PBS and blank NGs controls, Sap-EGFR/CD44-NGs greatly inhibited cell migration from the upper chamber of transwell to the lower side (Fig. 5C), which was significantly more effective than the mono-targeting Sap-CD44-NGs (Fig. 5D). Thus, Sap-EGFR/CD44-NGs can effectively inhibit 4T1 tumor cell migration.

3.4. In vivo therapeutic efficacy

The therapeutic efficacy of Sap-EGFR/CD44-NGs was examined using metastatic 4T1-luc breast tumor-bearing mice. Lung metastasis is the most frequently observed for 4T1 breast cancer (Su et al., 2016). Our results demonstrated that tumor metastasis in the lung was significantly suppressed by Sap-EGFR/CD44-NGs at a small dose of 3.33 nmol Sap equiv./kg (Fig. 6A), which was more effective than mono-targeting Sap-CD44-NGs (Fig. 6B). Increasing dosage of Sap-EGFR/CD44-NGs to 13.3 nmol Sap equiv./kg led to further reduced tumor photon flux in the lung. In contrast, mice treated with free saporin exhibited similar tumor metastasis to PBS and blank NGs groups, pointing out that carriers play a decisive role for application of saporin in vivo. The ex vivo bioluminescence imaging of lung harvested on day 13 further verified that Sap-EGFR/CD44-NGs offered the best inhibition of tumor metastasis (Fig. 6A). The counting of metastatic nodules in the lung showed that Sap-EGFR/CD44-NGs at a dosage of 3.33 nmol Sap equiv./kg caused significantly less metastasis than Sap-CD44-NGs (Fig. 6C). Further reduction of metastasis was induced by Sap-EGFR/CD44-NGs at 13.3 nmol Sap equiv./kg. On the contrary, free saporin, blank nanogels, and PBS groups displayed a high mean tumor nodule number of ca. 110. Fig. 6D shows that in contrast to free saporin, blank nanogels, and PBS groups that exhibited significantly increased total weight of lung and heart due to widespread metastasis and invasion (Wang et al., 2017), mice following the treatment with Sap-EGFR/CD44-NGs exhibited a lung and heart total weight of ca. 0.4–0.6 g, close to that of healthy mice.

Tumor metastasis and invasion in lung will cause weight loss in mice as a result of lung malfunction (Li et al., 2015; Wang et al., 2017). Fig. 7A shows that mice treated with free Sap displayed similar body weight loss (over 10%) to negative control groups (PBS and blank NGs) during the whole treatment period. In comparison, Sap-EGFR/CD44-NGs and Sap-CD44-NGs groups showed obviously less body weight loss. Notably, mice following the treatment with Sap-EGFR/CD44-NGs at 13.3 nmol Sap equiv./kg showed basically no body weight loss, indicating that they can effectively inhibit tumor metastasis without inducing systemic side effects. Blood analysis showed that mice treated with Sap-loaded NGs for 24 h had similar levels of red blood cells, white blood cells, hemoglobin, platelets, and hematocrit to PBS group (Fig. 7B), indicating that Sap-EGFR/CD44-NGs has excellent hemocompatability. The histological analysis demonstrated that unlike control groups (PBS and blank NGs) displaying significant damage of lung alveolar structure due to metastasis, lung tissue in mice treated with Sap-EGFR/CD44-NGs at 13.3 nmol Sap equiv./kg maintained defined alveolar structure (Fig. 7C). It should further be noted that serious metastasis was also detected in the liver for PBS and free Sap groups (Figs. 7C and S2), while little liver metastasis was detected in Sap-EGFR/CD44-NGs groups. Moreover, Sap-EGFR/CD44-NGs caused no damage of kidney and heart. These results point out that EGFR/CD44 dual-targeted NGs are an interesting platform to achieve efficient protein therapy for metastatic breast cancers.

4. Conclusions

We have demonstrated that CD44 and EGFR dual-targeted nanogels (EGFR/CD44-NGs) afford enhanced targetability and protein therapy for metastatic breast cancer in vivo. Notably, EGFR/CD44-NGs display more than 6-fold higher cellular uptake than CD44 mono-targeting nanogels (CD44-NGs) in CD44 and EGFR-positive metastatic 4T1 breast cancer cells. Saporin-loaded EGFR/CD44-NGs show obviously better antitumor effect and inhibition of cell migration as compared with saporin-loaded CD44-NGs. The therapeutic studies in metastatic 4T1-luc breast tumor-bearing mice have proved the concept that saporin-loaded EGFR/CD44-NGs can remarkably inhibit tumor metastasis to lung and liver tissues. EGFR and CD44 dual-targeted nanogels with superior specificity and enhanced protein delivery have appeared to be an interesting approach for treating metastatic breast cancers.

Conflict of interest

None.

Acknowledgments

This work was supported by the National Natural Science Foundation of China (NSFC 51773145, 51473110, and 51633005), and a Project Funded by the Priority Academic Program Development of Jiangsu Higher Education Institutions.

Appendix A. Supplementary data

Supplementary data to this article can be found online at https://doi.org/10.1016/j.ijpharm.2019.01.040.

References

Akishiba, M., Takeuchi, T., Kawaguchi, Y., Sakamoto, K., Yu, H.-H., Nakase, I., Takatani-Nakase, T., Madani, F., Graslund, A., Futaki, S., 2017. Cytosolic antibody delivery by lipid-sensitive endosomolytic peptide. Nat. Chem. 9, 751–761.
Chaffer, C.L., Weinberg, R.A., 2011. A perspective on cancer cell metastasis. Science 331, 1559–1564.
Chang, H., Lv, J., Gao, X., Wang, X., Wang, H., Chen, H., He, X., Li, L., Cheng, Y., 2017. Rational design of a polymer with robust efficacy for intracellular protein and peptide delivery. Nano Lett. 17, 1678–1684.
Chen, J., Ouyang, J., Chen, Q., Deng, C., Meng, F., Zhang, J., Cheng, R., Lang, Q., Zhong, Z., 2017b. EGFR and CD44 dual-targeted multifunctional hyaluronic acid nanogels boost protein delivery to ovarian and breast cancers in vitro and in vivo. ACS Appl. Mater. Interfaces 9, 24140–24147.
Chen, G., Wang, Y., Xie, R., Gong, S., 2017a. Tumor-targeted pH/redox dual-sensitive unimolecular nanoparticles for efficient siRNA delivery. J. Control. Release 259, 105–114.
Chen, G., Wang, Y., Wu, P., Zhou, Y., Yu, F., Zhu, C., Li, Z., Hang, Y., Wang, K., Li, J., Sun, M., Oupicky, D., 2018. Reversibly stabilized polycation nanoparticles for combination treatment of early- and late-stage metastatic breast cancer. ACS Nano 12, 6620–6636.
Chen, J., Zou, Y., Deng, C., Meng, F., Zhang, J., Zhong, Z., 2016. Multifunctional click hyaluronic acid nanogels for targeted protein delivery and effective cancer treatment in vivo. Chem. Mater. 28, 8792–8799.
Dutta, K., Hu, D., Zhao, B., Ribbe, A.E., Zhuang, J., Thayumanavan, S., 2017. Templated self-assembly of a covalent polymer network for intracellular protein delivery and taceless release. J. Am. Chem. Soc. 139, 5676–5679.
Fan, Y., Deng, C., Cheng, R., Meng, F., Zhong, Z., 2013. In situ forming hydrogels via catalyst-free and bioorthogonal “tetrazole-alkene” photo-click chemistry. Biomacromolecules 14, 2814–2821.
Gao, X., Zhang, J., Huang, Z., Zuo, T., Lu, Q., Wu, G., Shen, Q., 2017. Reducing interstitial fluid pressure and inhibiting pulmonary metastasis of breast cancer by gelatin modified cationic lipid nanoparticles. ACS Appl. Mater. Interfaces 9, 29457–29468.
Hamilton, A.M., Aidoudi-Ahmed, S., Sharma, S., Kotamraju, V.R., Foster, P.J., Sugahara, K.N., Ruoslahti, E., Rutt, B.K., 2015. Nanoparticles coated with the tumor-penetrating peptide iRGD reduce experimental breast cancer metastasis in the brain. J. Mol. Med. 93, 991–1001.
Han, X., Dong, X., Li, J., Wang, M., Luo, L., Li, Z., Lu, X., He, R., Xu, R., Gong, M., 2017. Free paclitaxel-loaded E-selectin binding peptide modified micelle self-assembled from hyaluronic acid-paclitaxel conjugate inhibit breast cancer metastasis in a murine model. Int. J. Pharm. 528, 33–46.
Hosseinzadeh, H., Atyabi, F., Varnamkhasti, B.S., Hosseinzadeh, R., Ostad, S.N., Ghahremani, M.H., Dinarvand, R., 2017. SN38 conjugated hyaluronic acid gold nanoparticles as a novel system against metastatic colon cancer cells. Int. J. Pharm. 526, 339–352.
Jiang, Y., Chen, J., Deng, C., Suuronen, E.J., Zhong, Z., 2014. Click hydrogels, microgels and nanogels: emerging platforms for drug delivery and tissue engineering. Biomaterials 35, 4969–4985.
Jiang, K., Chi, T., Li, T., Zheng, G., Fan, L., Liu, Y., Chen, X., Chen, S., Jia, L., Shao, J., 2017. A smart pH-responsive nano-carrier as a drug delivery system for the targeted delivery of ursolic acid: suppresses cancer growth and metastasis by modulating P53/

MMP-9/PTEN/CD44 mediated multiple signaling pathways. Nanoscale 9, 9428–9439.
Kreitman, R.J., Wilson, W.H., Bergeron, K., Raggio, M., Stetler-Stevenson, M., FitzGerald, D.J., Pastan, I., 2001. Efficacy of the anti-CD22 recombinant immunotoxin BL22 in chemotherapy-resistant hairy-cell leukemia. N. Engl. J. Med. 345, 241–247.
Landesman-Milo, D., Ramishetti, S., Peer, D., 2015. Nanomedicine as an emerging platform for metastatic lung cancer therapy. Cancer Metastasis Rev. 34, 291–301.
Li, M., Tang, Z., Zhang, Y., Lv, S., Li, Q., Chen, X., 2015. Targeted delivery of cisplatin by LHRH-peptide conjugated dextran nanoparticles suppresses breast cancer growth and metastasis. Acta Biomater. 18, 132–143.
Li, D., van Nostrum, C.F., Mastrobattista, E., Vermonden, T., Hennink, W.E., 2017. Nanogels for intracellular delivery of biotherapeutics. J. Control. Release 259, 16–28.
Liang, X., Shi, B., Wang, K., Fan, M., Jiao, D., Ao, J., Song, N., Wang, C., Gu, J., Li, Z., 2016. Development of self-assembling peptide nanovesicle with bilayers for enhanced EGFR-targeted drug and gene delivery. Biomaterials 82, 194–207.
Liang, D.-S., Zhang, W.-J., Wang, A.-T., Su, H.-T., Zhong, H.-J., Qi, X.-R., 2017. Treating metastatic triple negative breast cancer with CD44/neuropilin dual molecular targets of multifunctional nanoparticles. Biomaterials 137, 23–36.
Lim, D.G., Prim, R.E., Kang, E., Jeong, S.H., 2018. One-pot synthesis of dopamine-conjugated hyaluronic acid/polydopamine nanocomplexes to control protein drug release. Int. J. Pharm. 542, 288–296.
Liu, G., Choi, K.Y., Bhirde, A., Swierczewska, M., Yin, J., Lee, S.W., Park, J.H., Hong, J.I., Xie, J., Niu, G., Kiesewetter, D.O., Lee, S., Chen, X., 2012. Sticky nanoparticles: A platform for siRNA delivery by a bis(zinc(II) dipicolylamine)-functionalized, self-assembled nanoconjugate. Angew. Chem. Int. Ed. 51, 445–449.
Lluch, A., Alvarez, I., Munoz, M., Angel Segui, M., Tusquets, I., Garcia-Estevez, L., 2014. Treatment innovations for metastatic breast cancer: nanopartiele albumin-bound (NAB) technology targeted to tumors. Crit. Rev. Oncol. Hematol. 89, 62–72.
Mehlen, P., Puisieux, A., 2006. Metastasis: a question of life or death. Nat. Rev. Cancer 6, 449–458.
Morishige, M., Hashimoto, S., Ogawa, E., Toda, Y., Kotani, H., Hirose, M., Wei, S., Hashimoto, A., Yamada, A., Yano, H., Mazaki, Y., Kodama, H., Nio, Y., Manabe, T., Wada, H., Kobayashi, H., Sabe, H., 2008. GEP100 links epidermal growth factor receptor signalling to Arf6 activation to induce breast cancer invasion. Nat. Cell Biol. 10, 85–92.
Morshed, R.A., Muroski, M.E., Dai, Q., Wegscheid, M.L., Auffinger, B., Yu, D., Han, Y., Zhang, L., Wu, M., Cheng, Y., Lesniak, M.S., 2016. Cell-penetrating peptide-modified gold nanoparticles for the delivery of doxorubicin to brain metastatic breast cancer. Mol. Pharm. 13, 1843–1854.
Nan, X., Zhang, X., Liu, Y., Zhou, M., Chen, X., Zhang, X., 2017. Dual-targeted multifunctional nanoparticles for magnetic resonance imaging guided cancer diagnosis and therapy. ACS Appl. Mater. Interfaces 9, 9986–9995.
Obenauf, A.C., Massague, J., 2015. Surviving at a distance: organ specific metastasis. Trends Cancer 1, 76–91.
Qiao, C., Yang, J., Shen, Q., Liu, R., Li, Y., Shi, Y., Chen, J., Shen, Y., Xiao, Z., Weng, J., Zhang, X., 2018. Traceable nanoparticles with dual targeting and ROS response for RNAi-based immunochemotherapy of intracranial glioblastoma treatment. Adv. Mater. 30, 1705054.
Qiu, M., Zhang, Z., Wei, Y., Sun, H., Meng, F., Deng, C., Zhong, Z., 2018. Small-sized and robust chimaeric lipopepsomes: a simple and functional platform with high protein loading for targeted intracellular delivery of protein toxin in vivo. Chem. Mater. 30, 6831–6838.
Raghupathi, K., Eron, S.J., Anson, F., Hardy, J.A., Thayumanavan, S., 2017. Utilizing inverse emulsion polymerization to generate responsive nanogels for cytosolic protein delivery. Mol. Pharm. 14, 4515–4524.
Ramil, C.P., Lin, Q., 2014. Photoclick chemistry: a fluorogenic light-triggered in vivo ligation reaction. Curr. Opin. Chem. Biol. 21, 89–95.
Rao, N.V., Yoon, H.Y., Han, H.S., Ko, H., Son, S., Lee, M., Lee, H., Jo, D.-G., Kang, Y.M., Park, J.H., 2016. Recent developments in hyaluronic acid-based nanomedicine for targeted cancer treatment. Expert Opin. Drug Deliv. 13, 239–252.
Ravar, F., Saadat, E., Gholami, M., Dehghankelishadi, P., Mahdavi, M., Azami, S., Dorkoosh, F.A., 2016. Hyaluronic acid-coated liposomes for targeted delivery of paclitaxel, in-vitro characterization and in-vivo evaluation. J. Control. Release 229, 10–22.
Schroeder, A., Heller, D.A., Winslow, M.M., Dahlman, J.E., Pratt, G.W., Langer, R., Jacks, T., Anderson, D.G., 2012. Treating metastatic cancer with nanotechnology. Nat. Rev. Cancer 12, 39–50.
Su, J., Sun, H., Meng, Q., Yin, Q., Tang, S., Zhang, P., Chen, Y., Zhang, Z., Yu, H., Li, Y., 2016. Long circulation red-blood-cell-mimetic nanoparticles with peptide-enhanced tumor penetration for simultaneously inhibiting growth and lung metastasis of breast cancer. Adv. Funct. Mater. 26, 1243–1252.
Tang, S., Meng, Q., Sun, H., Su, J., Yin, Q., Zhang, Z., Yu, H., Chen, L., Gu, W., Li, Y., 2017. Dual pH-sensitive micelles with charge-switch for controlling cellular uptake and drug release to treat metastatic breast cancer. Biomaterials 114, 44–53.
Vermonden, T., Censi, R., Hennink, W.E., 2012. Hydrogels for protein delivery. Chem. Rev. 112, 2853–2888.
Walsh, G., 2014. Biopharmaceutical benchmarks 2014. Nat. Biotechnol. 32, 992–1000.
Wang, H., Agarvval, P., Zhao, S., Xu, R.X., Yu, J., Lu, X., He, X., 2015. Hyaluronic acid-decorated dual responsive nanoparticles of Pluronic F127, PLGA, and chitosan for targeted co-delivery of doxorubicin and irinotecan to eliminate cancer stem-like cells. Biomaterials 72, 74–89.
Wang, M., Alberti, K., Sun, S., Arellano, C.L., Xu, Q., 2014. Combinatorially designed lipid-like nanoparticles for intracellular delivery of cytotoxic protein for cancer therapy. Angew. Chem. Int. Ed. 53, 2893–2898.
Wang, H., Wang, R., Cai, K., He, H., Liu, Y., Yen, J., Wang, Z., Xu, M., Sun, Y., Zhou, X., Yin, Q., Tang, L., Dobrucki, I.T., Dobrucki, L.W., Chaney, E.J., Boppart, S.A., Fan, T.M., Lezmi, S., Chen, X., Yin, L., Cheng, J., 2017. Selective in vivo metabolic cell-labeling-mediated cancer targeting. Nat. Chem. Biol. 13, 415–424.
Wicki, A., Witzigmann, D., Balasubramanian, V., Huwyler, J., 2015. Nanomedicine in cancer therapy: challenges, opportunities, and clinical applications. J. Control. Release 200, 138–157.
Xu, R., Zhang, G., Mai, J., Deng, X., Segura-Ibarra, V., Wu, S., Shen, J., Liu, H., Hu, Z., Chen, L., Huang, Y., Koay, E., Huang, Y., Liu, J., Ensor, J.E., Blanco, E., Liu, X., Ferrari, M., Shen, H., 2016. An injectable nanoparticle generator enhances delivery of cancer therapeutics. Nat. Biotechnol. 34, 414–418.
Yae, T., Tsuchihashi, K., Ishimoto, T., Motohara, T., Yoshikawa, M., Yoshida, G.J., Wada, T., Masuko, T., Mogushi, K., Tanaka, H., Osawa, T., Kanki, Y., Minami, T., Aburatani, H., Ohmura, M., Kubo, A., Suematsu, M., Takahashi, K., Saya, H., Nagano, O., 2012. Alternative splicing of CD44 mRNA by ESRP1 enhances lung colonization of metastatic cancer cell. Nat. Commun. 3, 883.
Yang, J., Liao, D., Chen, C., Liu, Y., Chuang, T.-H., Xiang, R., Markowitz, D., Reisfeld, R.A., Luo, Y., 2013. Tumor-associated macrophages regulate murine breast cancer stem cells through a novel paracrine EGFR/Stat3/Sox-2 signaling pathway. Stem Cells 31, 248–258.
Yang, L., Mao, H., Wang, Y.A., Cao, Z., Peng, X., Wang, X., Duan, H., Ni, C., Yuan, Q., Adams, G., Smith, M.Q., Wood, W.C., Gao, X., Nie, S., 2009. Single chain epidermal growth factor receptor antibody conjugated nanoparticles for in vivo tumor targeting and imaging. Small 5, 235–243.
Yu, H., Guo, C., Feng, B., Liu, J., Chen, X., Wang, D., Teng, L., Li, Y., Yin, Q., Zhang, Z., Li, Y., 2016a. Triple-layered pH-responsive micelleplexes loaded with siRNA and cisplatin prodrug for NF-Kappa B targeted treatment of metastatic breast cancer. Theranostics 6, 14–27.
Yu, M., Wu, J., Shi, J., Farokhzad, O.C., 2016b. Nanotechnology for protein delivery: overview and perspectives. J. Control. Release 240, 24–37.
Zhang, X., Malhotra, S., Molina, M., Haag, R., 2015. Micro- and nanogels with labile crosslinks – from synthesis to biomedical applications. Chem. Soc. Rev. 44, 1948–1973.
Zhao, P., Yin, W., Wu, A., Tang, Y., Wang, J., Pan, Z., Lin, T., Zhang, M., Chen, B., Duan, Y., Huang, Y., 2017. Dual-targeting to cancer cells and M2 macrophages via biomimetic delivery of mannosylated albumin nanoparticles for drug-resistant cancer therapy. Adv. Funct. Mater. 27, 1700403.
Zhu, Y., Feijen, J., Zhong, Z., 2018. Dual-targeted nanomedicines for enhanced tumor treatment. Nano Today 18, 65–85.